Preprint typeset in JHEP style - HYPER VERSION

KIAS-P12026
HIP-2012-13/TH

Higgs Signatures in Inverse Seesaw Model at the LHC

Priyotosh Bandyopadhyay[a], **Eung Jin Chun**[b], **Hiroshi Okada**[b] **and Jong-Chul Park**[b]

[a] *Department of Physics and Helsinki Institute of Physics, University of Helsinki, FIN-00014, Helsinki, Finland*

[b] *Korea Institute for Advanced Study, Seoul 130-722, Korea*

Email: priyotosh.bandyopadhyay@helsinki.fi, ejchun@kias.re.kr, hokada@kias.re.kr, jcpark@kias.re.kr

Abstract: In the inverse seesaw mechanism where the spontaneously broken B-L symmetry induces tiny B-L violating Majorana masses for right-handed neutrinos, non-standard Higgs signatures can arise due to a possible Higgs doublet and singlet mixing and/or Higgs boson decays to a left- and right-handed neutrino. This leads to a remarkable feature of hadronically quiet di-lepton final states which can exhibit, in particular, lepton flavour violating signatures coming from flavour-dependent neutrino Yukawa couplings. In this process, one lepton coming from the right-handed decay could be soft enough can be missed by the trigger level cuts of CMS and ATLAS for the di-lepton plus missing energy signature. The prospects of such a signature are investigated for 8 TeV and 14 TeV center of mass energy of the LHC, taking the maximum value of the allowed neutrino Yukawa coupling and the right-handed neutrino mass of 100 GeV. A PYTHIA level simulation shows that the integrated luminosity of 10–20/fb and 1.6/fb for 8 TeV is required to observe the inclusive leptonic and lepton flavour violating signatures, respectively. For 14 TeV, the reach is more and a larger parameter space of the inverse seesaw model can be probed.

Keywords: Higgs, Inverse Seesaw, Collider Physics, Neutrino.

Contents

1. Introduction

A Higgs-like boson around 125 GeV has been observed by both CMS [1] and ATLAS [2] collaborations at the LHC. The 5σ discovery reach has been obtained for the Higgs boson to $\gamma\gamma$ mode for both CMS and ATLAS. The Higgs boson, if it is Standard Model (SM) like, can decay to di-leptonic final states through WW^* decay mode, which is of our interest in this paper. However, the significance in such a channel is still low: around 1.6σ for CMS [1] and 2.8σ for ATLAS [2]. The next question is, if such data will be able to provide information of the Higgs boson property, whether it is exactly of the SM or deviates from the SM. Non-standard Higgs structure arises in many extensions of the SM motivated by various theoretical reasoning and/or experimental requirements.

In the inverse seesaw mechanism [3, 4] explaining tiny neutrino mass, the seesaw sector couples to the SM sector with a Yukawa coupling of order-one and thus can lead to observable signatures at the LHC. A promising way to realize the inverse seesaw mechanism is to

consider a gauged $B-L$ symmetry which is broken spontaneously at TeV scale [5, 6]. In this case, the $B-L$ Higgs boson can mix with the SM Higgs boson which can change the SM Higgs boson signature at the LHC. Although the current LHC data strongly restricts such a mixing, we will try to take a conservative limit to maximize the mixing effect. Then the Higgs sector of the inverse seesaw model contains two Higgs bosons, a light and heavy one denoted by h and H, respectively. As these states are mixtures of the doublet and singlet Higgs states, their production is governed by the usual gluon fusion process of the doublet state.

On the other hand, the Higgs bosons can decay to the left- and right- handed neutrinos (denoted by ν and Ψ, respectively):

$$h, H \to \nu\Psi,\ \Psi\Psi \tag{1.1}$$

or $H \to hh$ depending on their masses. Then, the right-handed neutrino allows the decay modes:

$$\Psi \to lW,\ \nu Z \tag{1.2}$$

which can lead to hadronically quiet final states from the Higgs boson decay.[1] A careful observation shows that the lepton coming from the decay of the right-handed neutrino, Ψ could really be soft, depending on the mass difference between the right-handed neutrino and the W boson. We stress that, for some parameter points, this soft lepton could be already missed by ATLAS and CMS due to hard trigger level cuts for the leptons in the study of the Higgs boson to WW^* [9]. Another remarkable feature of the inverse seesaw is the possibility of lepton flavour violation as Ψ can dominantly decay to a specific lepton flavour, which occurs generically with hierarchical neutrino Yukawa couplings. In this paper, we analyze such non-standard Higgs signatures to discuss its discovery potential at the 8 and 14 TeV LHC.

The paper is organized as follows. In Section 2, we introduce the inverse seesaw model presenting the mass spectrum and the interaction vertices. The explicit form of all the interaction vertices of the model is shown in Appendix A. In Section 3, we discuss experimental constraints on the neutrino Yukawa coupling coming from the lepton universality as well as on the Higgs boson masses coming from the LEP and current LHC data. In Section 4, the benchmark points for our study are set up to calculate the branching ratios for the allowed decay model, and the final state phenomenology of each benchmark point is discussed. In Section 5, we analyze the missing and lepton p_T distributions and lepton multiplicity to suppress the standard di-boson background. Then, we discuss the discovery

[1] For related studies, see the recent works [7, 8].

potential of the signal events of two lepton (plus missing p_T) final states at the 8 and 14 TeV LHC. We conclude in Section 6.

2. Inverse seesaw model with U(1)$_{B-L}$

A natural way to realize the inverse seesaw mechanism is to introduce a $B-L$ gauge symmetry whose spontaneous breaking at the TeV scale generates a tiny $B-L$ breaking Majorana mass for right-handed neutrinos. The "minimal" field content implementing this idea would be as follows:

Particle	Q	u^c, d^c	L	e^c, N	S_1	S_2	Φ	χ
Y_{B-L}	1/3	-1/3	-1	1	-1/2	1/2	0	-1/2

(2.1)

where a pair of fermionic S_1 and S_2 is required to cancel the anomaly. The SM and $B-L$ Higgs bosons are denoted by Φ and χ, respectively. The gauge invariance of the model allows the leptonic sector Lagrangian in terms of the Weyl fermions as follows:

$$-\mathcal{L} = y_\ell L\Phi e^c + y_\nu L\Phi^c N + y_S N\chi S_1 + \frac{\lambda_{S_1}}{\Lambda}\chi^{\dagger 2}S_1^2 + \frac{\lambda_{S_2}}{\Lambda}\chi^2 S_2^2 + h.c.\,, \tag{2.2}$$

where $\Phi^c \equiv \epsilon\Phi^*$ and Λ is a cut-off scale. Note that the mass term S_1S_2 can be suppressed by introducing, e.g., a discrete symmetry Z_2 under which S_2 is odd and the others are even. After the symmetry breaking, $\chi = (\chi^0 + v')/\sqrt{2}$ and $\Phi = (\phi^+, \phi)^T$ with $\phi = (\phi^0 + v)/\sqrt{2}$, the neutrino sector can be written as

$$\mathcal{L}_m^\nu = m_D\nu' N + M_N N S_1 + \mu_S S_1^2 + h.c.\,, \tag{2.3}$$

where $m_D = y_\nu v/\sqrt{2}$, $M_N = y_S v'/\sqrt{2}$ and $\mu_S = \lambda_{S_1} v'^2/2\Lambda$. In the flavour basis $\{\nu', N, S_1\}$, the 3×3 neutrino mass matrix of one generation takes the form:

$$\begin{pmatrix} 0 & m_D & 0 \\ m_D & 0 & M_N \\ 0 & M_N & \mu_S \end{pmatrix}. \tag{2.4}$$

From the diagonalization of this mass matrix, one can find the light neutrino mass

$$m_\nu = \mu_S m_D^2/M_N^2\,. \tag{2.5}$$

Considering the constraint on m_D/M_N, which will be discussed in the following section, one can obtain $m_\nu \approx 0.1$ eV with the cut-off scale $\Lambda \approx 10^{15}$ GeV.

For the consideration of collider phenomenology, one can simply take the limit of $\mu_S = 0$. In this case, the active neutrino becomes massless and the other two heavy (Weyl)

neutrinos are degenerate to form a Dirac fermion. The mass basis is defined by the following rotation

$$\begin{pmatrix} \nu' \\ S_1 \end{pmatrix} = \begin{pmatrix} \cos\theta & \sin\theta \\ -\sin\theta & \cos\theta \end{pmatrix} \begin{pmatrix} \nu \\ N^c \end{pmatrix} \quad \text{where} \quad \sin\theta \equiv \frac{m_D}{\sqrt{m_D^2 + M_N^2}}, \tag{2.6}$$

where (N, N^c) form a Dirac fermion denoted by Ψ with the mass $m_\Psi = \sqrt{m_D^2 + M_N^2}$.

Now let us analyze the Higgs potential given by

$$V(\Phi, \chi) = m_1^2 \Phi^\dagger \Phi + m_2^2 \chi^\dagger \chi + \lambda_1 (\Phi^\dagger \Phi)^2 + \lambda_2 (\chi^\dagger \chi)^2 + \lambda_3 (\Phi^\dagger \Phi)(\chi^\dagger \chi). \tag{2.7}$$

After spontaneous breaking, the mass matrix is given by

$$M(\phi^0, \chi^0) = \begin{pmatrix} 2\lambda_1 v^2 & \lambda_3 v v' \\ \lambda_3 v v' & 2\lambda_2 v'^2 \end{pmatrix}, \tag{2.8}$$

where we use the stationary conditions:

$$\left.\frac{\partial V}{\partial \Phi}\right|_{v,v'} = 0 \to m_1^2 + \lambda_1 v^2 + \frac{1}{2}\lambda_3 v'^2 = 0, \tag{2.9}$$

$$\left.\frac{\partial V}{\partial \chi}\right|_{v,v'} = 0 \to m_2^2 + \lambda_2 v'^2 + \frac{1}{2}\lambda_3 v^2 = 0. \tag{2.10}$$

The neutral component of χ and ϕ mixes as follows:

$$\begin{pmatrix} \phi^0 \\ \chi^0 \end{pmatrix} = \begin{pmatrix} \cos\alpha & \sin\alpha \\ -\sin\alpha & \cos\alpha \end{pmatrix} \begin{pmatrix} h \\ H \end{pmatrix}, \tag{2.11}$$

where h (H) is the light (heavy) Higgs boson. The mass eigenvalues and the mixing angle are given by

$$m_{h,H}^2 = \lambda_1 v^2 + \lambda_2 v'^2 \mp \sqrt{(\lambda_1 v^2 - \lambda_2 v'^2)^2 + \lambda_3^2 v^2 v'^2}, \tag{2.12}$$

$$\tan 2\alpha = \frac{\lambda_3 v v'}{\lambda_2 v'^2 - \lambda_1 v^2}, \tag{2.13}$$

where $v = 246$ GeV. The most stringent bound on the value of the $B-L$ symmetry breaking scale v' comes from the LEP II data requiring $m_{Z'}/g_{B-L} = |Y_{B-L}^\chi| v' > 6$ TeV [10]. This tells us that $v' > 12$ TeV in our case. We set $v' = 12$ TeV for our analysis.

The interacting terms from the Higgs kinetic Lagrangian are given by

$$\begin{aligned} \mathcal{L}^K &= |D_\mu \Phi|^2 + |D_\mu \chi|^2 \\ &\supset \left[m_W^2 W_\mu^+ W^{-\mu} + \frac{1}{2} m_Z^2 Z_\mu Z^\mu \right] \left[1 + \frac{c_\alpha h + s_\alpha H}{v} \right]^2 \\ &\quad + \frac{1}{2} |Y_{B-L}^\chi|^2 m_{Z'}^2 Z'_\mu Z'^\mu \left[1 + \frac{-s_\alpha h + c_\alpha H}{v'} \right]^2 , \end{aligned} \tag{2.14}$$

where $m_Z = gv/(2c_{\theta_W})$ and $m_{Z'} = |Y^{\chi}_{B-L}| g_{B-L} v'$. The leptonic interaction Lagrangian is given by

$$\begin{aligned}
\mathcal{L}^{int.} &= \frac{y_{q_{u_i}}}{\sqrt{2}}(h\cos\alpha + H\sin\alpha)\bar{q}_{u_i}P_R q_{u_i} + \frac{y_{q_{b_i}}}{\sqrt{2}}(h\cos\alpha + H\sin\alpha)\bar{q}_{d_i}P_R q_{d_i} \\
&+ \frac{y_{\nu_i}}{\sqrt{2}}(h\cos\alpha + H\sin\alpha)\left[\cos\theta\bar{\Psi}_i P_L\nu_i + \sin\theta\bar{\Psi}_i P_L\Psi_i\right] \\
&+ \frac{y_{\ell_i}}{\sqrt{2}}(h\cos\alpha + H\sin\alpha)\bar{\ell}_i P_R\ell_i + \frac{y_{s_i}}{\sqrt{2}}(-h\sin\alpha + H\cos\alpha)[-\sin\theta\bar{\Psi}_i P_L\nu_i + \cos\theta\bar{\Psi}_i P_L\Psi_i] \\
&+ \frac{g}{\sqrt{2}}W^+_\mu\left[\cos\theta\bar{\nu}_i\gamma^\mu P_L(U_{MNS})_{ij}\ell_j + \sin\theta\bar{\Psi}_i\gamma^\mu P_L(U_{MNS})_{ij}\ell_j\right] \\
&+ \left(\frac{g}{2\cos\theta_W}Z_\mu\right)\left[\cos^2\theta\bar{\nu}_i\gamma^\mu P_L\nu_i + \sin^2\theta\bar{\Psi}_i\gamma^\mu P_L\Psi_i + \cos\theta\sin\theta(\bar{\nu}_i\gamma^\mu P_L\Psi_i + \bar{\Psi}_i\gamma^\mu P_L\nu_i)\right] \\
&+ h.c.\,, \qquad (2.15)
\end{aligned}$$

where $i = (e, \mu, \tau)$. and $(U_{MNS})_{ij}$ is Maki-Nakagawa-Sakata matrix [11]. All the interaction terms relevant for our analysis are summarized in Appendix A.

3. Experimental constraints on y_ν and the Higgs masses

The inverse seesaw model allows large neutrino Yukawa couplings y_ν. The most stringent constraint on y_ν comes from the electroweak precision data. From Table 8 of Ref. [12], one gets

$$\left|\frac{(m_D)_{e,\mu,\tau}}{M_N}\right| < (0.055,\ 0.057,\ 0.079)\,. \qquad (3.1)$$

This tells us that $(y_\nu)_i < c_i M_N/174\text{GeV}$ where c_i is the value for each flavour given in Eq. (3.1). To be consistent with this bound, we will take

$$\sin\theta_i \approx \frac{(m_D)_i}{M_N} = 0.05 \qquad (3.2)$$

for $i = e$ or μ for the collider study in the following sections.

The extra Higgs boson mass is constrained by the LEP and LHC data [13] as well as the current LHC data [2, 14]. In the inverse seesaw model, the Higgs production cross sections are suppressed by a factor of c^2_α and s^2_α for h and H, respectively. In addition, the decay branching fraction into SM particles is suppressed by a factor of $1 - \text{Br}(h/H \to \text{non-SM})$. If there exists a Higgs boson lighter than the 125 GeV Higgs, it is more singlet-like and an upper bound on c^2_α is put by the LEP data [13]. For the Higgs boson mass of 50 GeV, we find $c^2_\alpha \lesssim 0.05$. For a Higgs boson heavier than 125 GeV, the current LHC data [2, 14] puts an upper bound on s^2_α as shown in Fig. 1. For the 125 GeV Higgs boson, the overall signal strength measuring the deviation from the SM prediction is found to be

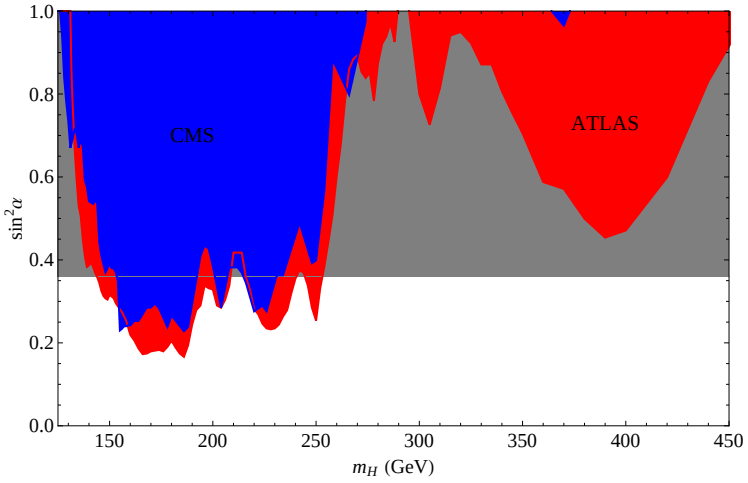

Figure 1: The heavy Higgs boson mass versus s_α^2. The red region is excluded by ATLAS, and the blue one is excluded by CMS. The gray region is excluded by the observation of the 125 GeV Higgs at CMS.

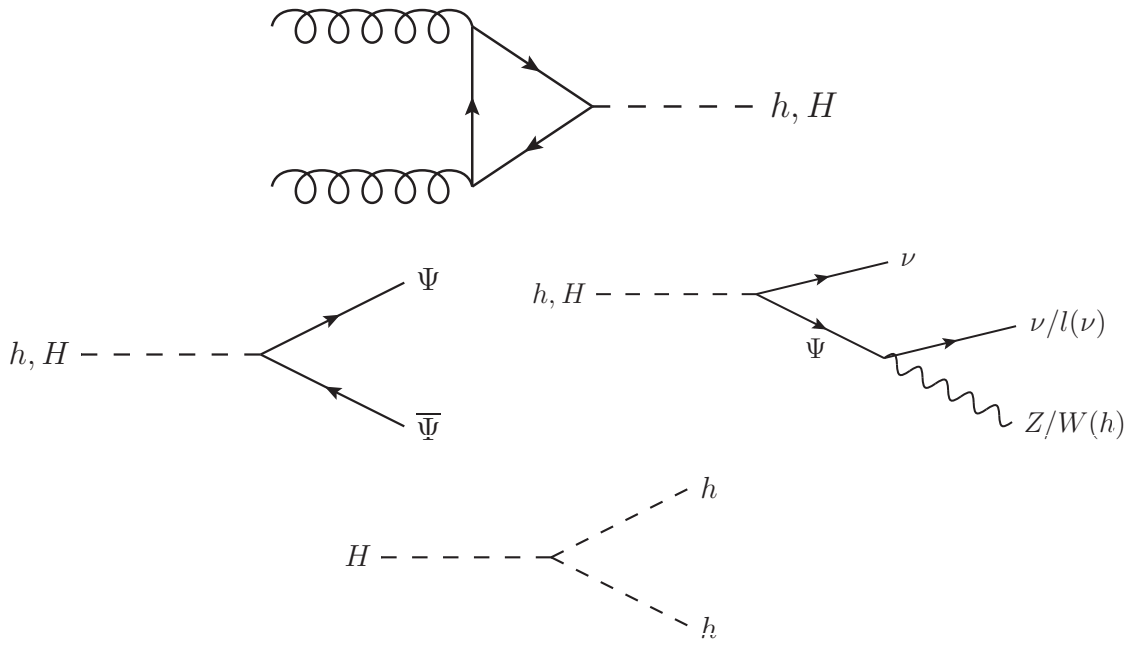

Figure 2: Feynman diagrams of the Higgs production via gluon fusion and the decay of Higgses.

$\mu = 1.4 \pm 0.3$ (ATLAS) [2] and $\mu = 0.87 \pm 0.23$ (CMS) [1]. Thus a non-standard Higgs boson contribution to the 125 GeV Higgs is strongly disfavoured. For our analysis, we will put a very conservative bound: $\mu > 0.64$, or $s_\alpha^2 < 0.36$ to see the maximized mixing effect.

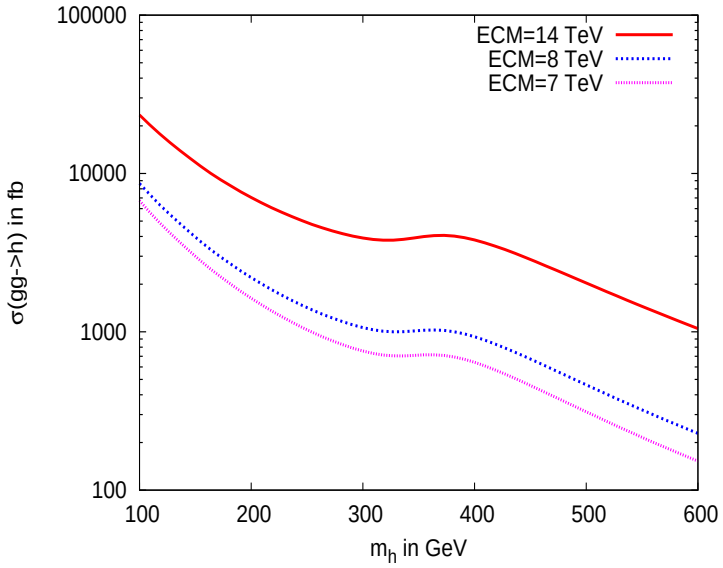

Figure 3: Standard Model Higgs production via gluon fusion at large Hadron collider for ECM=7, 8, 14 TeV. CTEQ5L PDF and $Q = \sqrt{\hat{S}}$ have been used. For our Higgs boson, we have to multiply by the corresponding rescaling factor $\sin^2\alpha$ or $\cos^2\alpha$.

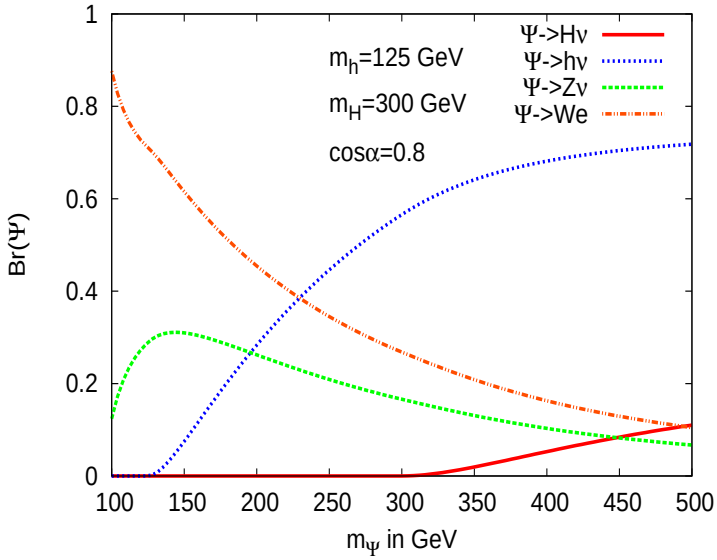

Figure 4: Variation of Ψ decay branching fraction with m_Ψ.

4. Benchmark Points and final state phenomenology

In this article, we are focusing on the gluon fusion process leading to a light/heavy Higgs bo-

son and its further decay to the right-handed neutrino and the corresponding phenomenology as stated in the introduction. Fig. 2 shows the Feynman diagram responsible for this process. Fig. 3 describes the variation of the Higgs production cross-section depending on the Higgs boson mass for 14 TeV and 8 TeV center of mass energy (ECM) at the LHC (and also for ECM=7 TeV as a reference). In our case, the cross-section for the light (heavy) Higgs boson will be scaled by $\cos^2\alpha$ ($\sin^2\alpha$) compared to the total Higgs production cross-section which is shown in Fig. 3. Fig. 4 shows the variation of the decay branching fraction of the right-handed neutrino, Ψ, with its mass for the fixed values of Higgs masses ($m_h = 125$ GeV, $m_H = 300$ GeV), $\cos\alpha = 0.8$ and λ couplings chosen for the case of BP4, which is defined later. We can read from the plot that the for low mass of the right-handed neutrino, it mostly decays to gauge bosons but for $m_\Psi \geq 250$ the decay branching to $h\nu$ dominates (always $> 50\%$).

Let us now select some relevant points for the phenomenological studies. For this purpose, we choose $\sin\theta \approx m_D/M_N = 0.05$ close to the current bound (3.1) for each generation. With this choice, we further consider two different options for the light Higgs boson.

1. Very low mass light Higgs (h): A very light (non-standard) Higgs boson mass (below 114 GeV) can still satisfy the corresponding LEP bound as discussed in the previous section. Keeping the the light Higgs mass fixed at 50 GeV we now choose two sets of points:

$$(m_H, m_\Psi, c_\alpha) = (125\ \text{GeV}, 100\ \text{GeV}, 0.1/0.25).$$

   Thus, for these two points, it is the heavier Higgs which stays in the discovery region of the LHC.

2. Light Higgs (h) in the LHC discovery region: Here we take $m_h = 125$ GeV and choose the following combinations:

$$(m_H, m_\Psi, c_\alpha) = (200/300\ \text{GeV}, 100\ \text{GeV}, 0.8).$$

   Note that the LHC bound (Fig. 1) sets a limit of $s_\alpha^2 \lesssim 0.33(0.36)$ for $m_H = 200(300)$ GeV. So, we made a generous choice of $c_\alpha = 0.8$ corresponding to $s_\alpha^2 = 0.36$.

Given the Higgs masses and $(v, v') = (246, 12000)$ GeV, the four-point Higgs couplings for each benchmark point in Table 1 can be found as follows:

1. BP1: $\lambda_1 = 0.128$, $\lambda_2 = 9.14 \times 10^{-6}$, $\lambda_3 = 4.42 \times 10^{-4}$,

Benchmark Points	m_h (GeV)	m_H (GeV)	m_Ψ (GeV)	$\cos\alpha$
BP1	50	125	100	0.1
BP2	50	125	100	0.25
BP3	125	200	100	0.8
BP4	125	300	100	0.8

Table 1: Benchmark points for common value of $\sin\theta = 0.05$.

2. BP2: $\lambda_1 = 0.122$, $\lambda_2 = 1.15 \times 10^{-5}$, $\lambda_3 = 1.08 \times 10^{-3}$,

3. BP3: $\lambda_1 = 0.202$, $\lambda_2 = 1.08 \times 10^{-4}$, $\lambda_3 = 3.96 \times 10^{-3}$,

4. BP4: $\lambda_1 = 0.350$, $\lambda_2 = 2.20 \times 10^{-4}$, $\lambda_3 = 1.21 \times 10^{-2}$.

Table 1 summarizes the benchmark points for our analysis. From Table 1, we can see that BP1 and BP2 correspond to low mass of the light Higgs that is not excluded by LEP [13] and the heavier Higgs mass is in the discovery region of the LHC. BP3 and BP4 correspond to relatively heavier light Higgs $m_h = 125$ GeV and heavy Higgses are 200 and 300 GeV, respectively.

In Table 2, the decay branching fractions of the heavy Higgs boson H are shown for the benchmark points. For BP1 and BP2, the heavy (125 GeV) Higgs decays to $\Psi\Psi$ is not open because of the unavailable phase space, but the decays to the light Higgs boson (h) pair is open. In case of BP3 where $m_H = 200$ GeV, the H decays to gauge bosons via one off-shell gauge boson as before, but the decay modes to $\Psi\Psi$ and hh are closed. In case of BP4, the heavy Higgs boson can decay to $\Psi\Psi$, as well as to hh. Table 3 shows the decay branching fractions for the light Higgs boson h for all the benchmark points. While the h decay to $\nu\Psi$ is closed in case of BP1 and BP2, it is open for BP3 and BP4 with a branching fraction $\sim 7\%$. Table 4 gives the decay branching fraction of Ψ for the four benchmark points. From the Table 4, it is clear that the right-handed neutrino mostly decays to gauge bosons.

In Table 5, we present the cross-sections of the Higgs boson production for the benchmark points with the center of mass energy of 14 and 8 TeV at the LHC, where we used CTEQ5L as PDF and $\sqrt{\hat{S}}$ as a scale.

Decay Modes	Branching Fraction			
	BP1	BP2	BP3	BP4
$\Psi\Psi$	-	-	-	0.002
$\nu\Psi$	0.06	0.03	0.0012	9.1×10^{-4}
$b\bar{b}$	0.57	0.27	0.004	0.002
$\tau\bar{\tau}$	0.06	0.03	4.0×10^{-4}	2.1×10^{-4}
hh	0.035	0.55	-	0.63
WW/WW^*	0.19	0.09	0.629	0.20
ZZ/ZZ^*	0.017	0.009	0.364	0.16
gg	0.046	0.021	0.001	0.002
$\gamma\gamma$	0.002	0.001	1.5×10^{-4}	7.6×10^{-5}

Table 2: Decay branching fraction of H for four benchmark points.

Let us now we discuss the various final sates for further phenomenological studies of the benchmark points. We focus on the contribution of the right-handed neutrino from the decays of heavy and light Higgses depending on the benchmark points. The final states are then determined from the decays of the right-handed neutrino.

4.1 BP1 & BP2

These two benchmark points correspond to the case of $m_h = 50$ GeV, forbidding the decay $h \to \nu\Psi$. The main decay modes of the lighter Higgs boson are $h \to bb$ and $\tau\tau$ leading to the final states: 2-b-jets + no $\not{p}_T$ and 2-τ-jets + no $\not{p}_T$. As the case with the usual Higgs search, it is very difficult to isolate the former signal from the QCD backgrounds. On the other hand, the τ-jet analysis could be interesting. As the lighter Higgs is very light in our case, it leads to very soft jets and thus the τ-jet tagging efficiency goes down. However, τ-jet tagging through one prong decay of τ can have better handle over the QCD background. Thus, a possibility of *2-τ-jets + no $\not{p}_T$* final state can still be important with a large accumulated luminosity.

The non-standard Higgs signature of our interest comes from the heavy Higgs which is SM-like with $m_H = 125$ GeV. As can be seen from Table 2 with $m_\Psi = 100$ GeV, the decay

Decay Modes	Branching Fraction			
	BP1	BP2	BP3	BP4
$\nu\Psi$	-	-	0.073	0.073
$b\bar{b}$	0.875	0.8756	0.58	0.58
$\tau\bar{\tau}$	0.076	0.076	0.06	0.06
WW	-	-	0.19	0.19
ZZ	-	-	0.017	0.017
gg	0.011	0.011	0.047	0.047
$\gamma\gamma$	0.003	0.003	0.002	0.002

Table 3: Decay branching fraction of h for four benchmark points.

Decay Modes	Branching Fraction			
	BP1	BP2	BP3	BP4
$h\nu$	0.068	0.167	-	-
$Z\nu_e$	0.116	0.103	0.124	0.124
W^+e	0.817	0.730	0.876	0.876

Table 4: Decay branching fraction of Ψ for four benchmark points.

$H \to \nu\Psi$ has a branching fraction $\sim 6\%$ for BP1 and 3% for BP2. Then, the produced right-handed neutrino (Ψ) will decay to gauge bosons as we can read from Table 4. This will lead to the prominent signal with respect to the backgrounds (see Fig. 5):

$$2\ell \ + \ 0\text{-jet} + \not{p}_T. \tag{4.1}$$

Hadronically quiet criteria along with two leptons kills the dangerous QCD and other hadronic backgrounds. The major SM hadronically quiet backgrounds come from the leptonic decays of WW, WZ and ZZ. Although there is a huge single vector boson production leading to two leptons; $pp \to \gamma^*/Z \to \ell^+\ell^-$, this does not carry any missing energy and can be efficiently reducible, specially with the Z mass window cut as will be discussed later.

	ECM=14 TeV		ECM=8 TeV	
	σ_h (fb)	σ_H (fb)	σ_h (fb)	σ_H (fb)
BP1	872.33	15869.3	370.18	5601.02
BP2	5452.06	15027.75	2313.63	5304.0
BP3	10258.94	2515.64	3620.86	782.89
BP4	10258.94	1386.12	3620.86	376.92

Table 5: $gg \to h/H$ production cross-section for four benchmark points for ECM=14 and 8 TeV, respectively, using CTEQ5L as PDF and $\sqrt{\hat{S}}$ as scale.

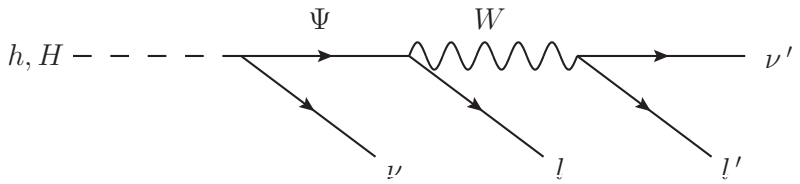

Figure 5: Decay topology of the Higgs(es) leading to the opposite sign lepton pair in the final state.

Let us remark that, in the case of BP2 with $\cos\alpha = 0.25$, the heavy Higgs (H) decay branching fraction to light Higgs (h) pair is about 55%. This will generate a $4b$ final state with no $\not{p}_T$. Plotting the invariant mass distribution of b-jet pairs, one could find a h peak although the signals would be challenged by the QCD background.

4.2 BP3 & BP4

For both BP3 and BP4, the light Higgs boson (h) can decay to $\nu\Psi$ with branching fraction 7.3%. This leads to a hadronically quiet di-leptonic final state (4.1), which was the case with the heavy Higgs for BP1 and BP2. The hadronically quiet 2ℓ scenario thus a generic signature for all the benchmark points.

On the other hand, the heavy Higgs (H) decay branching fraction to $\nu\Psi$ drops to $< 1\%$. In case of BP4, the heavy Higgs decay to $\Psi\Psi$ opens up but with very small branching fraction $\sim 0.2\%$. Even with such small branching fractions, the $\Psi\Psi$ and $\nu\Psi$ modes can still be probable due to the large production cross-section as in Table 5. BP4 allows the heavier Higgs decay mode $H \to hh$ with 63% of decay branching fraction, which is closed for BP3. The subsequent light Higgs decay to $\nu\Psi$ will open up an additional final

state:

$$4\ell \ + \ 0\text{-jet} + \not{p}_T. \tag{4.2}$$

The 4ℓ final state in case of benchmark points 3 and 4 also comes from the heavier Higgs decay to gauge boson pair. This implies that for heavier Higgs scenarios, either through gauge boson pairs or through the right-handed neutrino pair, $2\ell/4\ell$ final states without any hadronic activity are generic ones. In the following section, we will focus on these hadronically quiet two lepton final states for a collider simulation as the four lepton states turn out to be less significant.

5. Results

In this section, we go through a PYTHIA level analysis before presenting the final state results. `PYTHIA (version 6.4.22) [15]` has been used for the purpose of event generation. The model is implemented in Calchep [16] and the corresponding mass spectrum and decay branching fractions are generated. These are then fed to `PYTHIA` by using the SLHA interface [17]. Subsequent decays of the produced particles, hadronization and the collider analysis were performed using `PYTHIA`. We used `CTEQ5L` parton distribution function (PDF) [18] for the analysis. The renormalization/factorization scale Q was chosen to be the parton level center of mass energy, $\sqrt{\hat{S}}$. We also kept ISR, FSR and multiple interaction on for the analysis. We have used `PYCELL`, the toy calorimeter simulation provided in `PYTHIA`, with the following criteria:

I. The calorimeter coverage is $|\eta| < 4.5$ and the segmentation is given by $\Delta\eta \times \Delta\phi = 0.09 \times 0.09$ which resembles a generic LHC detector.

II. $\Delta R \equiv \sqrt{(\Delta\eta)^2 + (\Delta\phi)^2} = 0.5$ has been used in cone algorithm for jet finding.

III. $p_{T,min}^{jet} = 20$ GeV.

IV. No jet matches with a hard lepton in the event.

In addition, the following set of standard kinematic cuts were incorporated throughout:

1. $p_T^\ell \geq 5$ GeV and $|\eta|_\ell \leq 2.5$,

2. $|\eta|_j \leq 2.5$, $\Delta R_{\ell j} \geq 0.4$, $\Delta R_{\ell\ell} \geq 0.2$,

where $\Delta R_{\ell j}$ and $\Delta R_{\ell\ell}$ measure the lepton-jet and lepton-lepton isolation, respectively. Events with isolated leptons, having $p_T \geq 5$ GeV, are taken for the final state analysis.

Fig. 6 (left) plot shows the $\not{p}_T$ distribution for the model for BP4 and the SM background which is coming from the gauge boson pairs (WW, ZZ, ZW). In both cases, the origin of $\not{p}_T$ is neutrinos. In the case of background, it comes from the decay of the gauge bosons and thus it peaks around 45 GeV. On the other hand, in the case of signal, there are two different sources of neutrinos. The ones from the gauge bosons will behave similarly

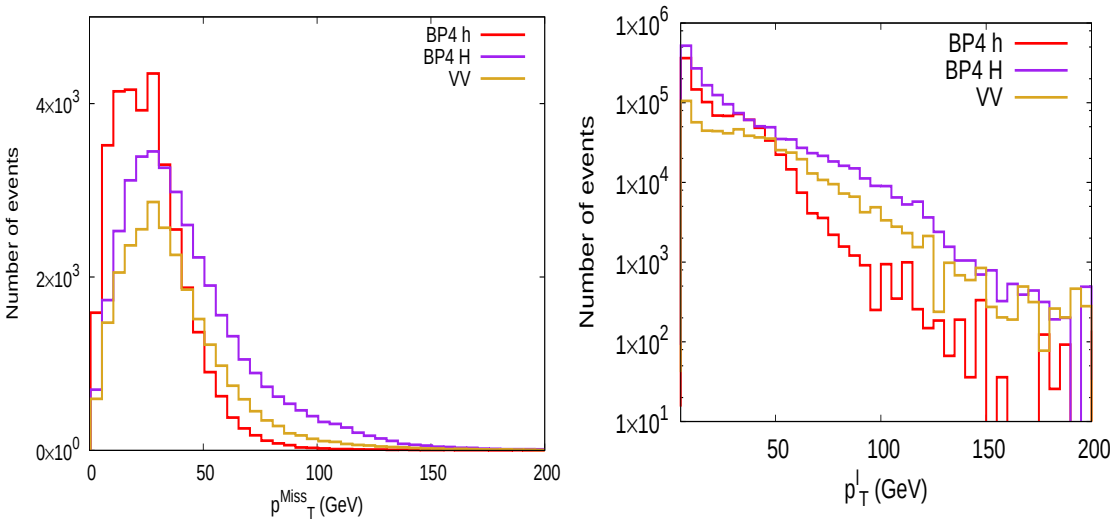

Figure 6: $\not{p}_T$ distribution (left) from heavy (H) and light (h) Higgses for BP4 and gauge boson pair background. The lepton p_T distribution (right) of signal×120 for BP4 heavier Higgs (H), signal×10 for the lighter Higgs (h) and background at 10 fb^{-1} integrated luminosity. Both of the plots are for ECM=8 TeV.

but the ones from the Higgs decay ($H \to \Psi\,\nu$) can have more p_T, depending on the mass difference between the Higgs and the right-handed neutrino. This results in a tail at higher $\not{p}_T$ (see Fig. 6 (left)) and some enhancement in the $\not{p}_T$ distribution for the heavier Higgs signal around 100 GeV for the case of benchmark point 4. In comparison, for the lighter Higgs (h), the tail dies below 100 GeV as expected. A requirement of minimum $\not{p}_T$ could be a good handle to kill the leptons coming from single Z, as charged lepton pair and neutrino pair come from Z decay in mutually exclusive manner. Higher $\not{p}_T$ cut $\geq$ 100 GeV could be a good handle to search for the existing heavy Higgs (H), however, we use soft $\not{p}_T$ cut while looking for 125 GeV Higgs as discussed in the next section.

Fig. 6 (right) plot shows the lepton p_T distribution coming from the signal (H and h) in the case of BP4 and from the gauge boson pair background, respectively. In the case of signal, the leptons that we will be looking for, have different origin. The one coming from the right-handed neutrino can be very soft due to the small mass gap between the right-handed neutrino and the W boson. The other one coming from W decay would be of SM like. We can see from the figure that the lepton from the signal, specially for the case of the heavier Higgs (H), is as hard as 125-150 GeV. This is because for BP4 the heavier Higgs mass is 300 GeV. The decay of such a particle to the light Higgs (h) pair or gauge boson pairs or though $\Psi\Psi$ or $\nu\Psi$ will share the momentum. Now the boosted decay products will transfer their momentum to their daughter leptons, which carry the

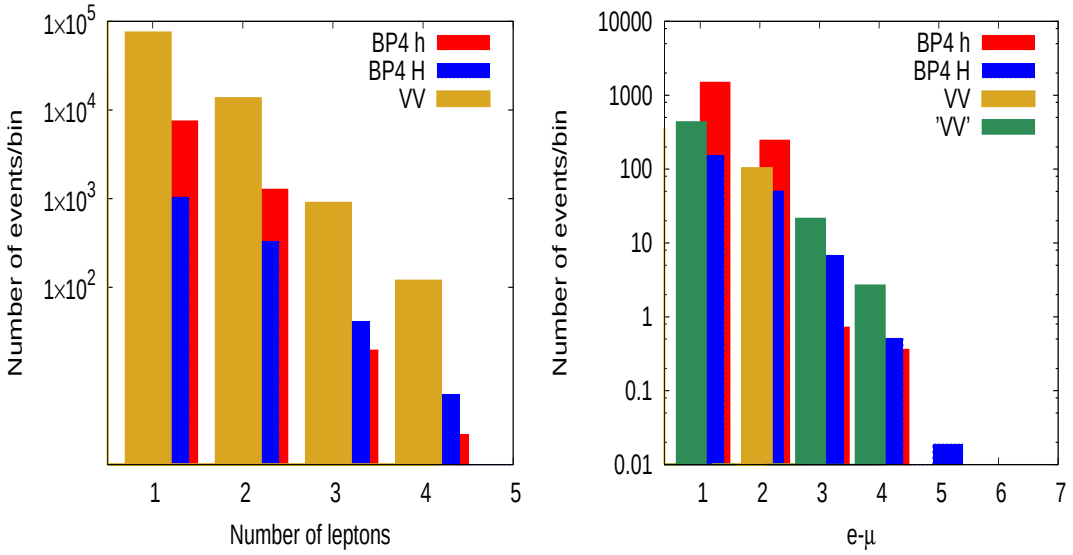

Figure 7: The left figure shows the lepton multiplicity distribution of signal for BP4 heavier Higgs (H), for the lighter Higgs (h) and background at 10 fb^{-1} integrated luminosity with ECM=8 TeV and the right figure shows $n_e - n_\mu$ ($n_\mu - n_e$) from the signal and di-boson background denoted by VV ('VV').

momentum depending on the decay channels. On the other hand, the lepton coming from the light Higgs (h) decay could be of very small momentum due to the small mass difference between the Higgs and the right-handed neutrino, which decays further to a lepton and W. Thus, the lepton p_T cuts, upper for the soft leptons and lower for hard leptons, will be crucial for signal event selection and reduction of the backgrounds.

Fig. 7 (left) describes the lepton multiplicity distribution for the signal for BP4 coming from the heavier Higgs and the lighter Higgs and also from the gauge boson pair backgrounds, respectively. The lepton multiplicity distribution is independent of the relative charge, i.e., same sign or opposite sign. We can see from the Fig. 7 (left) that the gauge boson pair backgrounds also have $2l$ and $4l$ final states from their decay to the charged leptons. Fig. 7 (right) describes the electron and muon number difference. The signal events contain more electrons for the signal from the decay of the right-handed neutrino as it is assumed to couple only to one flavour, i.e, the electron. On the other hand, for the background we expect the number to be very similar for e and μ case (that is, $|n_e - n_\mu| \ll n_e + n_\mu$). From Fig. 7 (left and right), we can see that the background is reduced a lot, in particular, for the case of $n_e - n_\mu$.

The main Standard Model backgrounds come from the di-boson production as discussed earlier. Apart from these, the Drell-Yan, i.e., $pp \to Z/\gamma^* \to \ell^+\ell^-$ could have

8TeV/10fb^{-1}		Signal				Background		
Final state		BP1	BP2	BP3	BP4	VV	Z/γ^*	$t\bar{t}$
S1 ($2l$)	h	0.09	0.23	269.03	269.03	3558.47	576.89	209.29
	H	352.02	154.34	43.75	4.60			
Significance		5.1	2.3	4.6	4.0			
14TeV/10fb^{-1}		Signal				Background		
Final state		BP1	BP2	BP3	BP4	VV	Z/γ^*	$t\bar{t}$
S1 ($2l$)	h	42.88	267.97	600.66	600.66	5774.59	3388.27	546.85
	H	820.44	324.60	117.48	14.34			
Significance		8.4	5.8	7.0	6.0			

Table 6: Number of events for 2ℓ final states for the benchmark points and the SM backgrounds at an integrated luminosity of 10 fb^{-1} with ECM = 8 and 14 TeV.

been a major background due to large cross-section but we find that this background is reducible one as it gives di-leptons without missing energy. We will also have a window cut $|M_{\ell,\ell} - M_Z| > 5$ GeV to further kill the dominant Z induced background. The $t\bar{t}$ background which is sub-dominant but still comparable to the signal event has also been implemented.

In the following two subsections, we present two sets of results. First, we discuss the hadronically quiet di-lepton scenario for inclusive flavour. Then, we address the case of lepton flavour violation, that is, $y_e \gg y_{\mu,\tau}$ (or $y_\mu \gg y_{e,\tau}$) for which the right-handed neutrino will decay only to eW and $\nu_e Z$ (or to μW and $\nu_\mu Z$).

5.1 Inclusive charged lepton signature

In this section, we discuss the flavour independent results which include both electron and muon, though we have lepton flavour violating coupling as the right-handed neutrino couples mostly to electrons, i.e., $y_e \gg y_{\mu,\tau}$. This study is also suitable for the case of $y_e = y_\mu$.

For BP1 and BP2, $h \to \nu\Psi$ decay is closed and h dominantly decays to $b\bar{b}$ or $\tau\bar{\tau}$ (see Table 3). The only contribution to 2ℓ comes from the semi-leptonic decays of b and τ. Thus, we do not have large contribution from the light Higgs in these cases. BP2 has more events than BP1 in the final state due to the larger cross-section compared to BP1. On the other hand, the heavier Higgs (H) can decay to $\nu\Psi$ with small branching fraction

($< 10\%$) as described in Table 2. Thus, the contributions are large enough due to large production cross-sections for the heavier Higgs in the cases of BP1 and BP2 as can be seen from Table 5. However, in the final event counting we expect BP1 should have twice the event of BP2, as the $\mathrm{Br}(H \to \Psi\nu) \sim 6\%$ in the case of BP1 and which is 3% in BP2 as cane be read from Table 2.

BP3 and BP4 are exactly same in terms of the lighter Higgs (h) having $m_h = 125$ GeV and $c_\alpha = 0.8$. This leads to the same decay branching to $\nu\Psi$, 7.3%, which results in large number of events for the final state. Also the gauge boson pairs contribute to the final states through off-shell decays of the lighter Higgs (h). In the case of the heavier Higgs (H), BP3 has the cross-section almost twice as large as BP4 (see Table 5), and the branching fraction to gauge boson pair is around $\sim 99\%$ for BP3 and $\sim 36\%$ for BP4. Unlike BP3, BP4 allows the decay $H \to hh$ with the branching fraction of 63%, which gives additional contribution to the di-lepton final state.

As we have discussed earlier, the lepton coming from the right-handed neutrino will be softer compared with that coming from $W^\pm$ (see Fig. 6). Thus, we demand the softer lepton with $p_T \leq 30$ GeV and the harder lepton with $p_T \geq 20$ GeV. This would help to reduce the SM di-lepton backgrounds, which generically come from gauge-boson decays. To kill the Z boson background , we reject the events with lepton invariant mass ($M_{\ell,\ell}$) around Z mass window, i.e., $|M_{\ell,\ell} - M_Z| \leq 5$ GeV (defined as $n_Z = 0$). On top of that, we also demand $p_T^{\ell_1} + p_T^{\ell_2} \leq 100$ GeV and $\not{p}_T \geq 30$ GeV. When we look for the signal coming from 125 GeV Higgs, we demand the sum of lepton p_T and $\not{p}_T$ should be less than 125 GeV. This cut will exclusively select events coming from 125 GeV Higgs. When we look for the events coming directly from heavier Higgs (H: $m_H = 200, 300$ GeV), the cut can be modified accordingly. In summary, the selection cut used for the inclusive $2l$ analysis is as follows:

$$\mathrm{S1}: \ \mathrm{n}_\ell = 2,\ \mathrm{n}_{\mathrm{jets}} = 0,\ \mathrm{n}_{\mathrm{Z}} = 0,\ \not{\mathrm{p}}_{\mathrm{T}} \geq 30\mathrm{GeV},\ \mathrm{P}_{\mathrm{T}}^{\ell} \leq 100\mathrm{GeV},\ \mathrm{M}_{\mathrm{eff}} \leq 125\mathrm{GeV} \qquad (5.1)$$

where $M_{\mathrm{eff}} = \sum(p_T^\ell + \not{p}_T)$ and $P_T^\ell = \sum p_T^\ell$.

In Table 6, we present all the event numbers from the signal (S) and background (B), and the significance defined by $S/\sqrt{S+B}$ for an integrated luminosity of 10 fb^{-1} at the 8 and 14 TeV LHC. We can see that the behaviour of BP1 and BP2 are complementary to that of BP3 and BP4 as the main contribution to the signal events come either from the heavy Higgs (H) for BP1 and BP2 or from the light Higgs (h) for BP3 and BP4, and the sum of two contributions are more or less the same except for BP2. The signal significance at the 8 TeV LHC reaches around 5σ except for BP2. In the case of the 14 TeV LHC, all the benchmark points reach high significance at an integrated luminosity of 10 fb^{-1}, which

8TeV/10fb^{-1}		Signal				Background		
Final state		BP1	BP2	BP3	BP4	VV	Z/γ^*	$t\bar{t}$
S2 ($2e$)	h	0.04	0.0	106.82	106.82	878.24	263.3	59.03
	H	122.38	55.96	10.44	1.58			
Significance		3.4	1.6	3.2	3.0			
14TeV/10fb^{-1}		Signal				Background		
Final state		BP1	BP2	BP3	BP4	VV	Z/γ^*	$t\bar{t}$
S2 ($2e$)	h	11.00	68.70	242.62	242.62	1480.36	1602.50	123.78
	H	311.83	125.48	26.67	3.81			
Significance		5.4	3.3	4.6	4.2			

Table 7: Number of events for $2e$ final states for the benchmark points and the SM backgrounds at an integrated luminosity of 10 fb^{-1} with ECM=8 TeV and 14 TeV.

implies that the parameter space of the inverse seesaw model can be readily probed at the LHC.

5.2 Lepton Flavour Violating signature

As mentioned earlier, much more significant search can be made if the right-handed neutrino has hierarchical Yukawa couplings and thus allows lepton flavour violation in its decay. Let us first consider the case that the right-handed neutrino couples only to electron. A comparative study of electron and muon lepton flavour will give a vital clue about the structure of the model as it can reduce significantly the SM background.

For this study, we select each flavour state keeping all the other cuts the same as in the previous section (5.1), and present results of our analysis for each signal channel labeled as

$$\text{S2} : 2e\,; \quad \text{S3} : 2\mu\,; \quad \text{S4} : 1e + 1\mu\,; \quad \text{and} \quad \text{S5} : 2e - 2\mu\,. \tag{5.2}$$

As expected, S5, corresponding to S2-S3, will give a novel signature to probe the inverse seesaw mechanism. Instead of S5, one could make an equivalent study with other lepton flavour violating final states such as $2 \cdot S2 - S4$ or $2 \cdot S3 - S4$.

Table 7 (8) shows the number of electron (muon) events for the signal for all the benchmark points and the backgrounds at an integrated luminosity of 10 fb^{-1} with center of mass energy of 8 and 14 TeV at the LHC. Unlike the lepton-universal gauge boson decay, the right-handed neutrino will produce only electron in the lW mode. For BP1 and

8TeV/10fb^{-1}		Signal				Background		
Final state		BP1	BP2	BP3	BP4	VV	Z/γ^*	$t\bar{t}$
S3 (2μ)	h	0.04	0.23	27.70	27.70	894.30	290.48	54.56
	H	49.84	22.80	11.57	1.07			
Significance		1.4	0.65	1.1	0.81			
14TeV/10fb^{-1}		Signal				Background		
Final state		BP1	BP2	BP3	BP4	VV	Z/γ^*	$t\bar{t}$
S3 (2μ)	h	11.03	68.97	58.46	58.46	1486.24	1761.64	127.48
	H	107.91	48.84	32.20	3.19			
Significance		2.0	2.0	1.5	1.0			

Table 8: Number of events for 2μ final states for the benchmark points and the SM backgrounds at an integrated luminosity of 10 fb^{-1} with ECM=8 and 14 TeV.

BP2, $h \to \nu\Psi$ decay is not open and thus we do not have the extra contribution to the electron events in the case of the light Higgs boson (h). This is clear from Table 7 and Table 8 where the electron and muon event numbers are similar as they come from the semi-leptonic decays of the decay products of the light Higgs (h). On the other hand, the heavy Higgs (H) with $m_H = 125$ GeV, can decay to $\nu\Psi$ and thus produces more electrons. The BP1 contribution is more than BP2 due to the larger branching fraction to $\nu\Psi$ and the cross-section of the former.

Similar is the case with the lighter Higgs (h) contribution for BP3 and BP4 as established in Table 7 and 8. The situation for BP3 is again a little different, as the heavier Higgs decay $H \to hh$ is not allowed and $H \to \nu\Psi$ branching fraction is very small $\sim 0.1\%$ (see Table 2). This ceases the extra electron contribution over muon for BP3. For BP4, heavier Higgs mass is 300 GeV and thus $H \to hh$ is allowed with 63% branching fraction. The lighter Higgs thus produced will decay to the right-handed neutrino as can be read from Table 3. Similar to the previous 2ℓ case, the complementary behaviour between the heavy and the light Higgs remains, i.e., for BP1 and BP2, it is the heavier Higgs which gives the lepton flavour violating signal generating extra electrons in the final state, whereas for BP3 and BP4, it is mainly the lighter Higgs. From Table 7 and 8, we can see that the significance for S3 is much smaller compared to S4 as expected.

For completeness, we also present the event numbers for the final state with $1e + 1\mu$, defined as S4. Table 9 shows the event numbers for S4. The Drell-Yan background is

8TeV/10fb^{-1}		Signal				Background		
Final state		BP1	BP2	BP3	BP4	VV	Z/γ^*	$t\bar{t}$
S4 $(1e+1\mu)$	h	0.02	0.00	134.51	134.51	1785.93	29.67	95.70
	H	179.79	75.58	21.75	1.94			
Significance		3.9	1.7	3.4	3.0			
14TeV/10fb^{-1}		Signal				Background		
Final state		BP1	BP2	BP3	BP4	VV	Z/γ^*	$t\bar{t}$
S4 $(1e+1\mu)$	h	20.85	130.30	299.56	299.56	2808.00	27.32	295.60
	H	400.70	150.28	58.61	7.35			
Significance		7.1	4.8	6.1	5.2			

Table 9: Number of events for $1e+1\mu$ final states for the benchmark points and the SM backgrounds at an integrated luminosity of 10 fb^{-1} with ECM=8 and 14 TeV.

8TeV/10fb^{-1}		Signal				Background		
Final state		BP1	BP2	BP3	BP4	VV	Z/γ^*	$t\bar{t}$
S5 $(2e-2\mu)$	h	0.00	-0.23	79.12	79.12	-16.07	-27.19	4.47
	H	72.53	33.15	-1.13	0.51			
Significance		12.5	-	12.5	12.5			
14TeV/10fb^{-1}		Signal				Background		
Final state		BP1	BP2	BP3	BP4	VV	Z/γ^*	$t\bar{t}$
S5 $(2e-2\mu)$	h	-4.36	-0.27	184.15	184.15	-5.87	-159.00	-3.69
	H	203.92	76.64	-5.53	0.62			
Significance		35.8	-	56.3	47.4			

Table 10: Number of events for $2e-2\mu$ final states for the benchmark points and the SM backgrounds at an integrated luminosity of 10 fb^{-1} with ECM=8 and 14 TeV.

reduced a lot due to the demand of different flavour leptons in the final state. The signal significance in this case is comparable to S2 ($2e$) and greater than S3 (2μ).

S2 ($2e$) from Table 7 and S3 (2μ) from Table 8 lead us to check the difference in the event numbers for the $2e$ and 2μ final states. As the SM backgrounds come from the

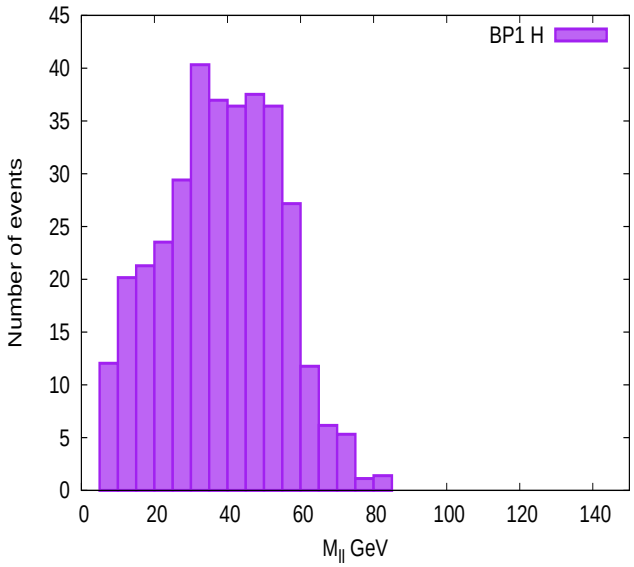

Figure 8: The opposite sign lepton invariant mass distribution with events with the same cut as S11 for BP1 heavier Higgs (H) at 10 fb^{-1} integrated luminosity with ECM=8 TeV.

flavour-blind decays of the gauge bosons, we expect that $2e - 2\mu$ event number will kill the background substantially giving only the extra electrons coming from the right-handed neutrino decays. This is the artifact of the lepton flavour violating right-handed neutrino coupling: $y_e \gg y_{\mu,\tau}$. Table 10 shows the difference in number of $2e$ and 2μ events (S5). We can again see that 125 GeV Higgs, which is the heavy Higgs (H) for BP1 and BP2 and the light Higgs (h) for BP3 and BP4, decays into more electrons than muons. The negative sign shows the events with more muons than electrons. From Table 10, we can see that $2e - 2\mu$ signal has a high significance except for BP2 for which the signal events are overshadowed by background for both 8TeV and 14TeV LHC at an integrated luminosity of 10 fb^{-1}.

Based on the above results, we can get the results for the opposite case where the right-handed neutrino couples only to the muon flavour: $y_\mu \gg y_{e,\tau}$. In this case, the signal significance drops due to the muon excess in the background: 7σ (10σ) for all points except BP2 with the 8 (14) TeV LHC which is still better than the inclusive flavour searches.

5.3 Mass measurement

Let us make a comment on the prospect of measuring the right-handed neutrino mass through the di-leptonic edge. Since we are looking for the decay chain of the right-handed neutrino; $\Psi \to lW \to l\bar{l}'\nu'$, the invariant mass of the final leptons gives rise to the famous

di-lepton edge [19]:

$$m_{\ell\ell}^{\max} = m_\Psi \sqrt{1 - \frac{m_W^2}{m_\Psi^2}} \sqrt{1 - \frac{m_\nu^2}{m_W^2}}. \tag{5.3}$$

As $m_\nu \approx 0$, the measurement of the maximum di-lepton invariant mass will tell us about the value of m_Ψ.

Fig. 8 shows the distribution of the di-lepton invariant mass for opposite sign di-leptons from the signals only under the same cuts as used for S1. Clearly, the edge can be seen at 60 GeV. Now reconstructing W through its hadron decay mode would be crucial in detecting the decay topology. For the signal, the decay topology via W boson indicates the mass of the right-handed neutrino at 100 GeV from the Eq. (5.3). Thus, the prescription described above not only gives a variable to get signal events over backgrounds but also results in a possibility to measure the mass of the right-handed neutrino. Analyzing the signal and background for events at 10 fb^{-1} of integrated luminosity, however, we find that it is very difficult to recognize the di-leptonic edge. We have to go to much higher luminosity to get a clear edge from the total distribution.

6. Conclusion

The inverse seesaw model introduces a tiny $B - L$ breaking Majorana mass of the right-handed neutrino which explains the smallness of the neutrino mass. This allows rather large neutrino Yukawa couplings through which the right-handed neutrinos can be produced at the LHC. We point out that the di-lepton final state with missing energy could be a smoking gun signal probing the Higgs and the right-handed neutrino of the inverse seesaw model. Furthermore, a novel signature of lepton flavor violation in these final states, such as the difference in the ee and $\mu\mu$ event numbers, may occur due to flavor-dependent neutrino Yukawa couplings. Taking the neutrino Yukawa coupling $y_{e,\mu} = 0.029$, which is close to the upper limit put by the lepton universality, and the right-handed neutrino mass of 100 GeV, we studied the LHC prospects to look for the inverse seesaw model in the four benchmark points. Performing a PYTHIA level simulation, it is found that the 5σ signal significance can be achieved with the integrated luminosity of $10 - 20$ fb^{-1} for the inclusive lepton (flavour-blind) signature, and $\lesssim 2$ fb^{-1} for the flavour violating signature at the 8 TeV LHC. We also pointed out that the observation of the di-lepton edge could shed light on the right-handed neutrino mass measurement. But it turns out to be hard to see the di-leptonic edge over the background with the nominal luminosity of the LHC14.

Acknowledgement: EJC was supported by the National Research Foundation of Korea (NRF) grant funded by the Korea government (MEST) (No. 20120001177). PB

thanks Korea Institute for Advanced Study for the travel support and local hospitality during some parts of this work.

A. Vertices

We write down all the relevant vertices below:

$$h - \bar{q}_{u(d)_i} - q_{u(d)_i} \ : \ \frac{y_{q_{u(d)_i}} \cos\alpha}{\sqrt{2}} P_R, \tag{A.1}$$

$$H - \bar{q}_{u(d)_i} - q_{u(d)_i} \ : \ \frac{y_{q_{u(d)_i}} \sin\alpha}{\sqrt{2}} P_R, \tag{A.2}$$

$$h - \bar{\ell}_i - \ell_i \ : \ \frac{y_{\ell_i} \cos\alpha}{\sqrt{2}} P_R, \tag{A.3}$$

$$H - \bar{\ell}_i - \ell_i \ : \ \frac{y_{\ell_i} \sin\alpha}{\sqrt{2}} P_R, \tag{A.4}$$

$$h - \bar{\Psi}_i - \nu_i \ : \ \frac{y_{\nu_i} \cos\alpha\cos\theta + y_{s_i} \sin\alpha\sin\theta}{\sqrt{2}} P_L, \tag{A.5}$$

$$H - \bar{\Psi}_i - \nu_i \ : \ \frac{y_{\nu_i} \sin\alpha\cos\theta - y_{s_i} \cos\alpha\sin\theta}{\sqrt{2}} P_L, \tag{A.6}$$

$$h - \bar{\Psi}_i - \Psi_i \ : \ \frac{y_{\nu_i} \cos\alpha\sin\theta - y_{s_i} \sin\alpha\cos\theta}{\sqrt{2}} P_L, \tag{A.7}$$

$$H - \bar{\Psi}_i - \Psi_i \ : \ \frac{y_{\nu_i} \sin\alpha\sin\theta + y_{s_i} \cos\alpha\cos\theta}{\sqrt{2}} P_L, \tag{A.8}$$

$$W^+ - \bar{\nu}_i - \ell_j \ : \ \frac{g\cos\theta (U_{MNS})_{ij}}{\sqrt{2}} P_L, \tag{A.9}$$

$$W^+ - \bar{\Psi}_i - \ell_j \ : \ \frac{g\sin\theta (U_{MNS})_{ij}}{\sqrt{2}} P_L, \tag{A.10}$$

$$Z - \bar{\nu}_i - \nu_i \ : \ \frac{g\cos^2\theta}{2\cos\theta_W} P_L, \tag{A.11}$$

$$Z - \bar{\Psi}_i - \Psi_i \ : \ \frac{g\sin^2\theta}{2\cos\theta_W} P_L, \tag{A.12}$$

$$Z - \bar{\nu}_i - \Psi_i (= Z - \bar{\Psi}_i - \nu_i) \ : \ \frac{g\cos\theta\sin\theta}{2\cos\theta_W} P_L, \tag{A.13}$$

$$h^4 \ : \ 6[\lambda_1 c_\alpha^4 + \lambda_2 s_\alpha^4 + \lambda_3 c_\alpha^2 s_\alpha^2], \tag{A.14}$$

$$H^4 \ : \ 6[\lambda_1 s_\alpha^4 + \lambda_2 c_\alpha^4 + \lambda_3 c_\alpha^2 s_\alpha^2], \tag{A.15}$$

$$h^2H^2 \ : \ 6(\lambda_1 + \lambda_2)c_\alpha^2 s_\alpha^2 + \lambda_3(s_\alpha^4 + c_\alpha^4 - 4s_\alpha^2 c_\alpha^2), \tag{A.16}$$

$$h^3H \ : \ (6\lambda_1 - 3\lambda_3)c_\alpha^3 s_\alpha + (-6\lambda_2 + 3\lambda_3)c_\alpha c_\alpha^3, \tag{A.17}$$

$$hH^3 \ : \ (-6\lambda_2 + 3\lambda_3)c_\alpha^3 s_\alpha + (6\lambda_1 - 3\lambda_3)c_\alpha c_\alpha^3, \tag{A.18}$$

$$h^3 \ : \ 6\lambda_1 v c_\alpha^3 - 6\lambda_2 v' s_\alpha^3 + 3\lambda_3(v s_\alpha - v' c_\alpha)s_\alpha c_\alpha, \tag{A.19}$$

$$H^3 \ : \ 6\lambda_1 v s_\alpha^3 + 6\lambda_2 v' c_\alpha^3 + 3\lambda_3(v c_\alpha + v' s_\alpha)s_\alpha c_\alpha, \tag{A.20}$$

$$hH^2 \ : \ 6\lambda_1 v c_\alpha s_\alpha^2 - 6\lambda_2 v' s_\alpha c_\alpha^2 + \lambda_3[2(-v s_\alpha + v' c_\alpha)s_\alpha c_\alpha - v' s_\alpha^3 + v c_\alpha^3], \tag{A.21}$$

$$h^2H \ : \ 6\lambda_1 v c_\alpha^2 s_\alpha + 6\lambda_2 v' s_\alpha^2 c_\alpha + \lambda_3[-2(v' s_\alpha + v c_\alpha)s_\alpha c_\alpha + v' c_\alpha^3 + v s_\alpha^3], \tag{A.22}$$

$$WWh \ : \ 2m_W^2 c_\alpha / v, \tag{A.23}$$

$$WWH \ : \ 2m_W^2 s_\alpha / v, \tag{A.24}$$

$$WWhh \ : \ 2m_W^2 c_\alpha^2 / v^2, \tag{A.25}$$

$$WWhH \ : \ 2m_W^2 s_\alpha c_\alpha / v^2, \tag{A.26}$$

$$WWHH \ : \ 2m_W^2 s_\alpha^2 / v^2, \tag{A.27}$$

$$ZZh \ : \ 2m_Z^2 c_\alpha / v, \tag{A.28}$$

$$ZZH \ : \ 2m_Z^2 s_\alpha / v, \tag{A.29}$$

$$ZZhh \ : \ 2m_Z^2 c_\alpha^2 / v^2, \tag{A.30}$$

$$ZZhH \ : \ 2m_Z^2 s_\alpha c_\alpha / v^2, \tag{A.31}$$

$$ZZHH \ : \ 2m_Z^2 s_\alpha^2 / v^2, \tag{A.32}$$

$$Z'Z'h \ : \ -2|Y_{B-L}^\chi|^2 m_{Z'}^2 \frac{s_\alpha}{v'}, \tag{A.33}$$

$$Z'Z'H \ : \ 2|Y_{B-L}^\chi|^2 m_{Z'}^2 \frac{c_\alpha}{v'}, \tag{A.34}$$

$$Z'Z'hh \ : \ 2|Y_{B-L}^\chi|^2 m_{Z'}^2 \frac{s_\alpha^2}{v'^2}, \tag{A.35}$$

$$Z'Z'hH \ : \ -2|Y_{B-L}^\chi|^2 m_{Z'}^2 s_\alpha \frac{c_\alpha}{v'^2}, \tag{A.36}$$

$$Z'Z'HH \ : \ 2|Y_{B-L}^\chi|^2 m_{Z'}^2 \frac{c_\alpha^2}{v'^2}, \tag{A.37}$$

where $Y_{B-L}^\chi = -1/2$ in our case.

References

[1] S. Chatrchyan *et al.* [CMS Collaboration], Phys. Lett. B **716** (2012) 30 [arXiv:1207.7235 [hep-ex]].

[2] G. Aad *et al.* [ATLAS Collaboration], Phys. Lett. B **716** (2012) 1 [arXiv:1207.7214 [hep-ex]].

[3] R. N. Mohapatra, Phys. Rev. Lett. **56**, 561 (1986).

[4] R. N. Mohapatra and J. W. F. Valle, Phys. Rev. D **34**, 1642 (1986).

[5] S. Khalil, J. Phys. G **35**, 055001 (2008) [arXiv:hep-ph/0611205].

[6] W. Abdallah, A. Awad, S. Khalil and H. Okada, Eur. Phys. J. C , 72:2108 (2012) [arXiv:1105.1047 [hep-ph]].

[7] P. S. B. Dev, R. Franceschini and R. N. Mohapatra, arXiv:1207.2756 [hep-ph].

[8] C. G. Cely, A. Ibarra, E. Molinaro and S. T. Petcov, arXiv:1208.3654 [hep-ph].

[9] CMS Collaboration, Phys. Lett. B **710** (2012) 91 [arXiv:1202.1489 [hep-ex]]; ATLAS Collaboration, arXiv:1206.0756, ATLAS-CONF-2012-098.

[10] K. Nakamura *et al.* [Particle Data Group], J. Phys. G **37**, 075021 (2010).

[11] Z. Maki, M. Nakagawa and S. Sakata, Prog. Theor. Phys. **28**, 870 (1962).

[12] F. del Aguila, J. de Blas and M. Perez-Victoria, Phys. Rev. D **78**, 013010 (2008) [arXiv:0803.4008 [hep-ph]].

[13] R. Barate *et al.* [LEP Working Group for Higgs boson searches and ALEPH Collaboration and and], Phys. Lett. B **565**, 61 (2003) [arXiv:hep-ex/0306033].

[14] S. Chatrchyan *et al.* [CMS Collaboration], Phys. Lett. B **710** (2012) 26 [arXiv:1202.1488 [hep-ex]].

[15] T. Sjostrand, S. Mrenna and P. Z. Skands, JHEP **0605**, 026 (2006).

[16] A. Pukhov, hep-ph/0412191.

[17] P. Z. Skands *et al.*, JHEP **0407**, 036 (2004).

[18] H. L. Lai *et al.* [CTEQ Collaboration], Eur. Phys. J. C **12**, 375 (2000); J. Pumplin *et al.*, JHEP **0207**, 012 (2002).

[19] C. G. Lester and D. J. Summers, Phys. Lett. B **463** (1999) 99 [hep-ph/9906349].